ORIGINAL ARTICLE

Effectiveness of [^{67}Cu]Cu-trastuzumab as a theranostic against HER2-positive breast cancer

Jessica Pougoue Ketchemen[1] · Fabrice Ngoh Njotu[1,2] · Hanan Babeker[1,2] · Stephen Ahenkorah[3,4] · Anjong Florence Tikum[1] · Emmanuel Nwangele[1,2] · Nikita Henning[1] · Frederik Cleeren[4] · Humphrey Fonge[1,5]

Abstract

Purpose To evaluate the imaging and therapeutic properties (theranostic) of ^{67}Cu-labeled anti-human epidermal growth factor receptor II (HER2) monoclonal antibody trastuzumab against HER2-positive breast cancer (BC).

Methods We conjugated trastuzumab with *p*-SCN-Bn-NOTA, 3p-*C*-NETA-NCS, or *p*-SCN-Bn-DOTA, and radiolabeled with [^{67}Cu]CuCl$_2$. Immunoconjugate internalization was evaluated in BT-474, JIMT-1 and MCF-7 BC cells. In vitro stability was studied in human serum (HS) and Phosphate Buffered Saline (PBS). Flow cytometry, radioligand binding and immunoreactive fraction assays were carried out. ImmunoSPECT imaging of [^{67}Cu]Cu-NOTA-trastuzumab was done in mice bearing BT-474, JIMT-1 and MCF-7 xenografts. Pharmacokinetic was studied in healthy Balb/c mice while dosimetry was done in both healthy Balb/c and in athymic nude mice bearing JIMT-1 xenograft. The therapeutic effectiveness of [^{67}Cu]Cu-NOTA-trastuzumab was evaluated in mice bearing BT-474 and JIMT-1 xenografts after a single intravenous (i.v.) injection of ~ 16.8 MBq.

Results Pure immunoconjugates and radioimmunoconjugates (> 95%) were obtained. Internalization was HER2 density-dependent with highest internalization observed with NOTA-trastuzumab. After 5 days, in vitro stabilities were $97 \pm 1.7\%$, $31 \pm 6.2\%$, and $28 \pm 4\%$ in HS, and $79 \pm 3.5\%$, $94 \pm 1.2\%$, and $86 \pm 2.3\%$ in PBS for [^{67}Cu]Cu-NOTA-trastuzumab, [^{67}Cu]Cu-3p-*C*-NETA-trastuzumab and [^{67}Cu]Cu-DOTA-trastuzumab, respectively. [^{67}Cu]Cu-NOTA-trastuzumab was chosen for further evaluation. BT-474 flow cytometry showed low K$_D$, 8.2 ± 0.2 nM for trastuzumab vs 26.5 ± 1.6 nM for NOTA-trastuzumab. There were 2.9 NOTA molecules per trastuzumab molecule. Radioligand binding assay showed a low K$_D$ of 2.1 ± 0.4 nM and immunoreactive fraction of 69.3 ± 0.9. Highest uptake of [^{67}Cu]Cu-NOTA-trastuzumab was observed in JIMT-1 ($33.9 \pm 5.5\%$ IA/g) and BT-474 ($33.1 \pm 10.6\%$ IA/g) xenograft at 120 h post injection (p.i.). Effectiveness of the radio-immunoconjugate was also expressed as percent tumor growth inhibition (%TGI). [^{67}Cu]Cu-NOTA-trastuzumab was more effective than trastuzumab against BT-474 xenografts (78% vs 54% TGI after 28 days), and JIMT-1 xenografts (90% vs 23% TGI after 19 days). Mean survival of [^{67}Cu]Cu-NOTA-trastuzumab, trastuzumab and saline treated groups were > 90, 77 and 72 days for BT-474 xenografts, while that of JIMT-1 were 78, 24, and 20 days, respectively.

Conclusion [^{67}Cu]Cu-NOTA-trastuzumab is a promising theranostic agent against HER2-positive BC.

Keywords ^{67}Cu · *p*-SCN-Bn-NOTA · Theranostics · HER2-positive breast cancer · Dosimetry

✉ Humphrey Fonge
humphrey.fonge@usask.ca

1 Department of Medical Imaging, College of Medicine, University of Saskatchewan, Saskatoon, SK S7N 0W8, Canada

2 Department of Pathology and Lab. Medicine, College of Medicine, University of Saskatchewan, 107 Wiggins Rd, Saskatoon, SK S7N 5A2, Canada

3 NURA Research Group, Belgian Nuclear Research Center (SCK CEN), Mol, Belgium

4 Radiopharmaceutical Research, Department of Pharmacy and Pharmacology, University of Leuven, Leuven, Belgium

5 Department of Medical Imaging, Royal University Hospital Saskatoon, Saskatoon, SK S7N 0W8, Canada

Introduction

Breast cancer (BC) is the second leading cause of cancer deaths in females, accounting for 15.5% of all cancer-related deaths [1]. Human epidermal growth factor receptor type 2 (HER2) is an oncogene that is amplified and overexpressed in 25—30% of BC, and other cancers of epithelial origin including ovarian, gastric, esophageal and endometrial cancers [2]. Patients with HER2-positive BC have poor prognosis, high recurrence rates, disease aggressiveness, metastatic progression, and overall low survival rates [3–5].

Anti-HER2 monoclonal antibodies trastuzumab, pertuzumab, margetuximab, and antibody drug conjugates (ADCs) ado-trastuzumab emtansine (T-DM1), trastuzumab-deruxtecan (T-DXd), as well as tyrosine kinase inhibitors lapatinib, neratinib, pyrotinib, tucatinib are all approved against HER2-positive BC [6]. These targeted therapeutics have resulted in significant gains in survival for patients compared with standard of care consisting of chemotherapeutics, radiotherapy, and surgery [7]. Despite these gains, de novo and acquired resistance to these agents is common in patients [7].

Radioimmunotherapy (RIT) and peptide receptor radionuclide therapy (PRRT) which employ respectively, monoclonal antibodies and peptides as delivery vehicles for potent radionuclides to cancer cells are very promising therapeutic approaches. RIT and PRRT have shown benefits in patients in several recent clinical trials against different solid tumors [8]. Alpha-particle labeled [212Pb]Pb-TCMC-trastuzumab [TCMC:1,4,7,10-tetraaza-1,4,7,10-tetra(2-carbamoylmethyl) cyclododecane], β−-emitting [177Lu]Lu-DOTA-trastuzumab [DOTA: 1,4,7,10-tetraazacyclododecane-1,4,7,10-tetraacetic acid], and [177Lu]Lu-DOTA-ABY-027 (a second generation affibody molecule $Z_{HER2:2891}$) are RIT agents against HER2-positive BC [9–13]. In vivo, these RITs have been extensively investigated in models of HER2-positive colorectal and ovarian cancer, but not in BC. They showed tumor control rates but no complete remissions were observed even in trastuzumab sensitive models. A significant disadvantage of [212Pb]Pb is that the high energy gammas result in very high organ doses which is very dose limiting [14]. The in vivo effectiveness of alpha particle-labeled [227Th]Th-DOTA-trastuzumab has also been evaluated in models of trastuzumab-sensitive ovarian cancer [15] and BC [16]. However, radiochemical yields of DOTA chelated [227Th]Th is < 5% making such a RIT undevelopable. Thorium-227 chelation has been a challenge historically not until Abou et al. recently presented data on a stable chelator with high radiochemical yield [17] using ofatumumab monoclonal antibody in a lymphoma model.

In precision oncology, a theranostic approach whereby a radiolabeled imaging agent in conjunction with an imaging modality such as PET/SPECT is used for diagnosis & staging, accurate dosimetry evaluation, evaluation of response to treatments, and/or selection of patients that would benefit from treatment using the radiolabeled therapeutic agent has resulted in significantly better overall management of cancers. Recent examples such as [68Ga]Ga-DOTA-TATE/ [177Lu]Lu-DOTA-TATE or 68Ga-PSMA/177Lu-PSMA agents have resulted in unprecedented improvements in the management of neuroendocrine tumors (NETs) and prostate cancer, respectively [18].

Trastuzumab radiolabeled with zirconium-89 (89Zr), indium-111 (111In), and copper-64 (64Cu) have been evaluated in patients with HER2-positive BC, and demonstrated to be safe and useful as imaging agents [19]. [177Lu]Lu-DOTA-trastuzumab was evaluated in phase 1 with HER2-positive BC, and showed uptake in [18F]FDG avid lesions [19]. However, image quality was poor as the gamma branching ratio of 177Lu [E_γ = 113 keV (6.6%), 208 keV (11%)] does not offer images of diagnostic quality. The therapeutic effectiveness of 177Lu is attributed to its decay characteristics ($t_{1/2}$ = 6.65 day, β− = 100%, $E_{\beta^- mean}$ = 134 keV, $E_{\beta^- max}$ = 497 keV) which gives its ionizing β−-emissions a tumor penetration depth of 2 mm. The use of other radiometals such as 89Zr, 64Cu or 111In (similar half-lives as an imaging pair for the therapeutic 177Lu) as imaging pair for [177Lu]Lu-DOTA-trastuzumab therapy is far from ideal as these radiometals in spite of their near ideal decay properties either require the use of different chelators for complexation compared with 177Lu or may exhibit very different pharmacokinetic profiles in vivo [20, 21]. Therefore, there is a need for matched theranostic pair or a theranostic single.

Copper has two medically useful radionuclides 67Cu ($t_{1/2}$ = 2.58 day) and 64Cu ($t_{1/2}$ = 12.7 h) which are increasingly being exploited for their theranostics potentials. This surge for 67Cu is due to recent advancements in the production of clinical grade radionuclide [22, 23]. While the positron-emitting 64Cu complexed with Sar-TATE and DOTA-TATE has proven to be an excellent PET imaging isotope for diagnosis and dosimetry prior to [67Cu]Cu-Sar-TATE and [177Lu]Lu-DOTA-TATE radionuclide therapies, 67Cu on the other hand, can be used as a theranostic single [24–27]. 67Cu (β− = 100%, $E_{\beta^- mean}$ = 141 keV, $E_{\beta^- max}$ = 562 keV) decays by β−-emissions with higher mean and maximal energies compared to those of 177Lu (β− = 100%, $E_{\beta^- mean}$ = 134 keV, $E_{\beta^- max}$ = 497 keV) and, therefore is expected to have similar or better therapeutic effects compared with 177Lu. In theory, these characteristics would make [67Cu]Cu-trastuzumab theranostic better or similar compared with [177Lu]Lu-trastuzumab.

Therefore, the current project was undertaken to develop and evaluate [67Cu]Cu-labeled trastuzumab as a theranostic against HER2-positive BC. To develop 67Cu-labeled trastuzumab, we first evaluated the complexation of 67Cu using the

bifunctional chelators (BFCs) 3p-*C*-NETA-NCS, *p*-SCN-Bn-DOTA and *p*-SCN-Bn-NOTA. The most stable construct was used to evaluate the effectiveness of the theranostic in HER2-positive BC in vitro and in vivo.

Materials and methods

Cell lines, reagents, and xenografts

Human BC cell lines BT-474 (RRID:CVCL_0179) and MCF-7 (RRID:CVCL_0031) with high and low HER2 expression, respectively, were purchased from American Type Culture Collection (ATCC) (Rockville, MD). JIMT-1 (RRID:CVCL_2077) cell line was kindly provided by Dr. Victor Jeffrey Leyton (School of Pharmaceutical Sciences, University of Ottawa, Ottawa ON). Cell culture was done in monolayers in their respective media, which were supplemented with 10% fetal bovine serum (FBS) (Biochrom, Sigma-Aldrich, St Louis, MO) and 1% penicillin–streptomycin (Hyclone Laboratories, Logan UT) at 37 °C in a humidified atmosphere with 5% carbon dioxide (CO_2). BT-474 and JIMT-1 were cultured in high glucose Dulbecco's Modified Eagle's Medium (DMEM) (Hyclone Laboratories, Logan UT) and MCF-7 was cultured in Eagle's Minimum Essential Medium (EMEM) (ATCC, catalogue #: 30–2003). Cell lines were mycoplasma-free, and authenticated using short tandem repeat (STR) profiling at the Centre for Applied Genomics (Hospital for SickKids, Toronto, ON).

Research grade trastuzumab was purchased from Ichorbio (Catalogue #: ICH4013, Oxford UK). The bifunctional chelators (BFCs) *p*-SCN-Bn-NOTA, and *p*-SCN-Bn-DOTA were purchased from Macrocyclics, Plano TX) while 3p-*C*-NETA-NCS was generously provided by the Laboratory for Radiopharmaceutical Research, KU Leuven (Leuven Belgium).

Female athymic Balb/c nude mice (n = 3–4/group with tumor volume of 62.5—256 mm^3, body weights of 20–22 g) were used for immunoSPECT/CT imaging and biodistribution. Radioimmunotherapy was carried out using female athymic Balb/c nude mice (n = 5–9/group with tumor volume of 54.1—81.6 mm^3, and body weights of 21–33 g at the start of the therapy). We used healthy female Balb/c mice (n = 4/group, body weights of 20–22 g) for pharmacokinetic studies. Dosimetry was carried out in both healthy Balb/c and in athymic nude mice bearing JIMT-1 xenograft (n = 4/time point). Mice were purchased from Charles River (Saint-Constant, QC) and were at least 6 weeks of age. The University of Saskatchewan Animal Care Committee (UACC) (protocol # 20220021) approved protocols and guidelines were followed. The animals were maintained at 12 h light and 12 h dark cycles, in a humidity-controlled vivarium, and were fed ad libitum with food (Lab Diet, St. Louis, MO) and water. All mice had at least one week of acclimatization before being assigned to the various groups. BT-474 and MCF-7 mice xenografts were developed by inoculating the nude mice with 17-β-estradiol pellets (0.36 mg, 90-days sustained release, Innovative Research of America, Sarasota, FL) at the left back neck region. Three to five days after inoculation, 10–20 million cells of BT-474 and MCF-7 in 100 μL suspension of a 1:1 mixture of complete growth media and Matrigel matrix basement membrane (catalogue # 08-774-391, Fisher Scientific, Ottawa ON) were subcutaneously injected in the right and left hind limb respectively [28]. About 10 million JIMT-1 cells were injected in the same manner but without pellet pre-inoculation. Mice were monitored daily, and the size of the tumors was determined using a digital caliper, and the volume was estimated using volume = ½(length x width^2) [29].

Conjugation with BFCs, characterization, and internalization of immunoconjugates

Prior to labeling with [^{67}Cu]CuCl$_2$, trastuzumab was conjugated with the various BFCs following lab SOPs [30]. The purified conjugates were stored at -80 °C before labeling. The purity of the respective conjugates was determined using a size-exclusion HPLC (SEC-HPLC) Waters 2487 Dual λ Absorbance Detector, XBridge® BEH 200 A SEC 3.5 μm 7.8 × 150 nm column (Waters Corporation, Milford, MA), and an Agilent 2100 Bioanalyzer system (Agilent High Sensitivity Protein 250 Kit- catalogue# 5067-1575) following the manufacturer's protocol.

The isotopic dilution method was used to determine the number of NOTA molecules per antibody [31]. A series of standardized CuCl$_2$ dilutions (starting concentration of 500 μM were prepared to react with NOTA-trastuzumab. For each tube 3 MBq of [^{67}Cu]CuCl$_2$, neutralized with 14 μL of 150 mM ammonium acetate pH 5.8-6.0, and 3 μL NOTA-trastuzumab (6.6 μM) were added. After 30 min of incubation at 37 °C, 2 μL of the reaction mixture in each tube was spotted for instant thin layer chromatography (iTLC) analysis. The number of NOTA groups was calculated based on a graph of the percentage yield versus the concentration of the standard CuCl$_2$ analyzed using GraphPad Prism (GraphPad Software, LA Jolla, CA).

To assess internalization of immunoconjugates, HER2-positive BT-474, JIMT-1 and MCF-7 cells were seeded in a flat bottom 96 well plates and incubated for ~ 48 h before adding the immunoconjugates. The IncuCyte® FabFluor reagent (Essen BioScience, Ann Arbor, MI) was conjugated with either trastuzumab or its conjugates with *p*-SCN-Bn-NOTA, 3p-*C*-NETA-NCS, and *p*-SCN-Bn-DOTA at a molar ratio of 1:3 in complete growth media, for 15 min at 37 °C. Equal volumes (50 μL) of media and FabFluor-labeled antibody were then added to the cells in triplicates prior to imaging using IncuCyte® S3 live-cell imager (Essen

BioScience, Ann Arbor, MI) [32]. The area under the curve (AUC (μm^2h)) was determined from the red object area versus time curve using GraphPad Prism.

Radiolabeling with $[^{67}Cu]CuCl_2$ or $[^{177}Lu]LuCl_3$ and stability of radioimmunoconjugates

^{67}Cu-chloride ($[^{67}Cu]CuCl_2$) was produced using an electron linear accelerator at the Canadian Isotope Innovations Corp (CIIC, Saskatoon, SK), while $[^{177}Lu]LuCl_3$ was obtained from McMaster Nuclear Reactor Facility (Nuclear Research Building, McMaster University, Hamilton, ON), and the radiolabeling was done following lab SOP. 150 mM ammonium acetate buffer was added to $[^{67}Cu]CuCl_2$ solution to obtain a pH between 5.8-6.0 prior to the addition of the respective immunoconjugates (NOTA-trastuzumab, 3p-*C*-NETA-trastuzumab, and DOTA-trastuzumab) at a specific activity of 1 MBq/μg. Similar procedure was used for $[^{177}Lu]LuCl_3$ labeling of DOTA-trastuzumab. The reaction mixtures were incubated for at least 30 min at 37 °C. After incubation, the reactions were cooled to 25 °C, and the radiochemical yield and purity were determined using iTLC with 20 mM sodium citrate buffer (pH 5.0) as eluent. Radio SEC-HPLC was used to confirm the radiochemical purity and radiochemical efficiency of all the radioimmunoconjugates as described above.

The in vitro stability of $[^{67}Cu]Cu$-NOTA-trastuzumab, $[^{67}Cu]Cu$-3p-*C*-NETA-trastuzumab, and $[^{67}Cu]Cu$-DOTA-trastuzumab was studied in HS and PBS at 37 °C for 5 days (n = 3). About 50 μL of each radioimmunoconjugate was added to a 1.5 mL vial containing either 450 μL of HS or PBS under constant gentle shaking. To determine the stability, 5 μL samples were drawn for iTLC analysis at specific time points (10 min, 24, 48, 72, and 120 h).

Flow cytometry

The binding of NOTA-trastuzumab and trastuzumab to BT-474 (high HER2 density/cell), JIMT-1 (medium HER2 density/cell), and MCF-7 (low HER2 density/cell) cells was performed in triplicates using lab SOP [33]. To determine the binding affinity of non-radioactive copper-labeled trastuzumab (Cu^{stand}-NOTA-trastuzumab), we first performed a "cold" labelling of NOTA-trastuzumab. Briefly, a reaction mixture of 60 μL of ammonium acetate, 54 μL of NOTA-trastuzumab and 7 μL of standardised $CuCl_2$ was incubated at 37 ºC for 30 min. Purified Cu^{stand}-NOTA-trastuzumab was then used for binding assay with a starting concentration of 1 μM following lab SOP. Binding was studied using the CytoFLEX flow cytometer (Beckman Coulter, Indianapolis, USA) and analyzed using FlowJo (version 10.8.2; FlowJo LLC, Ashland, USA), and GraphPad Prism Version 9 to obtain the binding constant (K_D), maximum number of receptor/cell (B_{max}), and half maximal effective concentration (EC_{50}).

Radioligand binding assay, and immunoreactivity

Evaluation of HER2 binding affinity of $[^{67}Cu]Cu$-NOTA-trastuzumab was done using HER2-positive BT-474 cells as reported [32]. About 0.3 X 10^6 cells in PBS were added in tubes and incubated with increasing concentrations of radiolabeled antibody (0.02-6.25 nM in 100 μL) for 4 h at 4 °C (total binding-TB). Nonspecific binding (NSB) was determined in parallel by incubating cells in another set of tubes with 100-fold molar excess of cold trastuzumab for at least 30 min at 4 °C prior to the addition of $[^{67}Cu]Cu$-NOTA-trastuzumab. Each group of cells (n = 3) was washed three times with PBS and centrifuge at 161 g to collect the supernatant. The counts of respective cell pellets and washes were measured using the gamma counter (Wallac Wizard 1480, PerkinElmer, Waltham, MA) [32]. Specific binding was calculated by subtracting NSB from TB. The data was analyzed using a non-linear regression curve with one-site binding equation on GraphPad Prism version 9 to determine the K_D and B_{max}. The immunoreactive fraction of $[^{67}Cu]Cu$-NOTA-trastuzumab was determined using Lindmo et al. protocol [34].

Pharmacokinetics and radiation dosimetry

Pharmacokinetics (PK) was studied in healthy female Balb/c mice (n = 4) after injection with ~ 6 MBq/6 μg per mouse of $[^{67}Cu]Cu$-NOTA-trastuzumab via a tail vein. Blood samples were collected using sodium heparinized capillary tubes at different times post injection (p.i.), and radioactivity in the tubes was counted using the gamma counter (Wallac Wizard 1480, PerkinElmer, Waltham, MA) and expressed as percentage injected activity per milliliter (% IA/mL). Various PK parameters were calculated by fitting a curve of blood radioactivity versus time to a two-compartment model with intravenous bolus input [35].

The radioactivity of normal tissues and blood was determined in healthy female Balb/c, and in female athymic Balb/c nude mice bearing JIMT-1 xenograft (n = 4/time point). Mice were injected with 5-6 MBq of $[^{67}Cu]Cu$-NOTA-trastuzumab followed by biodistribution at 1, 6, 24, 48, 120, 168 h (healthy Balb/c mice) or at 1, 6, 24, 120 h p.i. (mice bearing JIMT-1 xenograft). Body organs were harvested, weighed, and counted for radioactivity in a gamma counter. Blood and tissue uptake were expressed as percentage injected activity per gram (%IA/g) and a graph was plotted. The mouse biodistribution (%IA/g) data was extrapolated to human data (%IA) using the formular % IA (human) = % IA/g (mouse) x total body weight of mouse (in kg) x mass of human organ (in g) / total body weight of

human (in kg). For each organ, this was plotted against sampling time, and used to obtain an estimate of the residence time of the agent in the organ in MBq-h/MBq, represented by the area under the time-activity function integrated to infinity (complete decay) of the ^{67}Cu. The residence time was fitted into the OLINDA kinetics model (OLINDA/EXM V2.2, Hermes Medical Solutions Montreal QC) to generate absorbed doses in units of mSv/MBq of ^{67}Cu radioimmunoconjugate (RIC) administered [36, 37].

ImmunoSPECT/CT imaging and biodistribution

For immunoSPECT/CT imaging, female athymic Balb/c nude mice (n = 3/group) bearing BT-474 (right flank) and MCF-7 (left flank) xenografts, and another group bearing JIMT-1 (right flank) were injected via tail vein using 10–11 MBq of [^{67}Cu]Cu-NOTA-trastuzumab. Imaging studies were performed three times at 24, 48 and 120 h p.i. using the Vector^{4}CT scanner (MILabs B.V., Utrecht, The Netherlands), and analyzed using PMOD 3.7 software (PMOD, Davos, Switzerland). ImmunoSPECT scans were acquired in a list-mode data format using a high-energy ultra-high resolution (HE-UHR-1.0 mm) mouse/rat pinhole collimator. A pixel-based order-sunset expectation maximization (POS-EM) algorithm was used for the CT scans. At the end of imaging (120 h p.i.), the mice were sacrificed for biodistribution studies. Additional group of female athymic Balb/c nude mice (n = 3–4) bearing BT-474, JIMT-1 and MCF-7 tumors were injected via a tail vein with [^{67}Cu]Cu-NOTA-trastuzumab and sacrificed at 24 h p.i. for biodistribution studies. The radioactivity in blood and organs were counted using the gamma counter and expressed as %IA/g.

Radioimmunotherapy

When HER2-positive BT-474 and JIMT-1 tumor xenografts had reached an average size of 66 mm^3 (54.1–81.6 mm^3), female athymic Balb/c nude mice were randomized into three different groups per xenograft model (n = 5–9/group). For each xenograft model, there were no significant differences in tumor volume between groups at the start of therapy. BT-474 and JIMT-1 tumor bearing mice were treated with a single dose of [^{67}Cu]Cu-NOTA-trastuzumab (~ 16.8 MBq) injected via a tail vein, while positive treated control group received trastuzumab (5 mg/kg). The non-treated group was injected with saline. Another group of mice bearing JIMT-1 xenograft (n = 8) were treated using a single dose of ~ 16.8 MBq of [^{177}Lu]Lu-DOTA-trastuzumab, which was intended to be used to compare with [^{67}Cu]Cu-NOTA-trastuzumab. The study was terminated when tumor volume reached ≥ 600 mm^3 (these were not allowed to reach the conventional 1500 mm^3 because they frequently ulcerated necessitating euthanasia), or when the health conditions of the mice were compromised, and this was used to determine survival in the different groups using a Kaplan Meier curve. Individual body weight of each mouse was recorded during the quarantine (every other day) and experimental period.

Statistics

Data are presented as mean ± standard error of the mean (SEM) of at least 3 replicated experiments. Percentage tumor growth inhibition (%TGI) of test groups was determined relative to control groups using the formular $(1-\Delta T/\Delta C) \times 100$, where ΔT and ΔC are the differences between final and initial tumor volumes of test and control groups, respectively. A one-way ANOVA, and two-way ANOVA with Bonferroni or Dunnett post hoc test was used to determine the statistical significance between groups. GraphPad Prism Version 9 was used to generate all figures.

Results

Characterization and internalization of immunoconjugates

More than 98% pure homogenous trastuzumab conjugates (NOTA-trastuzumab, 3p-*C*-NETA-trastuzumab, and DOTA-trastuzumab) were obtained following conjugation using the different BFCs as shown by the bioanalyzer (Supplementary Fig. S1A) and SEC-HPLC (Supplementary Fig. S1B). Putative structure of the immunoconjugates is presented (Supplementary Fig. S1D). These pure conjugates were then used to study the internalization kinetics prior to ^{67}Cu radiolabeling, and in vitro stability studies.

In all BT-474, JIMT-1 and MCF-7 cells, we observed a rapid time-dependent increase in red fluorescence (internalization of immunoconjugates into the lysosomes and endosomes) for naked trastuzumab and respective chelator-conjugated trastuzumab from 2 to 48 h. The highest fluorescence was observed with NOTA-trastuzumab in both BT-474 and MCF-7 cell lines, however, for JIMT-1 cells, 3p-*C*-NETA-trastuzumab had the highest fluorescence (Supplementary Fig. S2A, B and C). Internalization was dependent on receptor density and was far greater for BT-474 compared with JIMT-1 and MCF-7. The AUC (μm^{2}h) of the internalization-time curve of NOTA-trastuzumab was greater than trastuzumab in both BT-474 (27.8% higher ($p = 0.0001$)) and MCF-7 (23.9% higher), showing an enhancement of internalization of NOTA conjugate compared with those of 3p-*C*-NETA and DOTA conjugate. The least internalization was observed with control anti-CD20 IgG (rituximab) in BT-474 and MCF-7. In JIMT-1 cells with medium HER2 expression and resistant to naked trastuzumab showed no significant difference in internalization between trastuzumab, NOTA-trastuzumab or

DOTA-trastuzumab ($p > 0.9999$). (Fig. 1A, B and C). These effects are delineated in the phase contrast images (Supplementary Fig. S2D).

^{67}Cu and ^{177}Lu radiolabeling and in vitro stability of radiocomplexes

Radiolabeling of NOTA-trastuzumab, 3p-*C*-NETA-trastuzumab, and DOTA-trastuzumab with [^{67}Cu]CuCl$_2$ or DOTA-trastuzumab with [^{177}Lu]LuCl$_3$ at a specific activity of 1 MBq/µg with heating at 37 °C for 30 min resulted in good radiochemical yields (RCY > 95%) and purity (RCP > 95%) for [^{67}Cu]Cu-NOTA-trastuzumab, and [^{177}Lu]Lu-DOTA-trastuzumab, but additional purification was needed for [^{67}Cu]Cu-3p-*C*-NETA-trastuzumab and [^{67}Cu]

Cu-DOTA-trastuzumab to obtain high purity as confirmed using radio SEC-HPLC (Supplementary Fig. S1B and C).

In vitro stability was studied at different time points by analyzing the RCP of the radioimmunoconjugates after incubation with HS or PBS. After 5 days, in vitro stability in HS of [^{67}Cu]Cu-NOTA-trastuzumab (RCP 97 ± 1.7%,) was > [^{67}Cu]Cu-3p-*C*-NETA-trastuzumab (RCP 31 ± 6.2%) > [^{67}Cu]Cu-DOTA-trastuzumab (RCP 28 ± 4%), with the NOTA-radioimmunoconjugate being significantly ($p < 0.0001$) more stable that the 3p-*C*-NETA and DOTA constructs (Fig. 1D). In PBS, the order of stability after 5-days was [^{67}Cu]Cu-3p-*C*-NETA-trastuzumab (RCP 94 ± 1.2%) > [^{67}Cu]Cu-DOTA-trastuzumab (RCP 86 ± 2.3%) > [^{67}Cu]Cu-NOTA-trastuzumab (RCP 79 ± 3.5%) (Fig. 1E). [^{67}Cu]Cu-NOTA-trastuzumab was chosen for
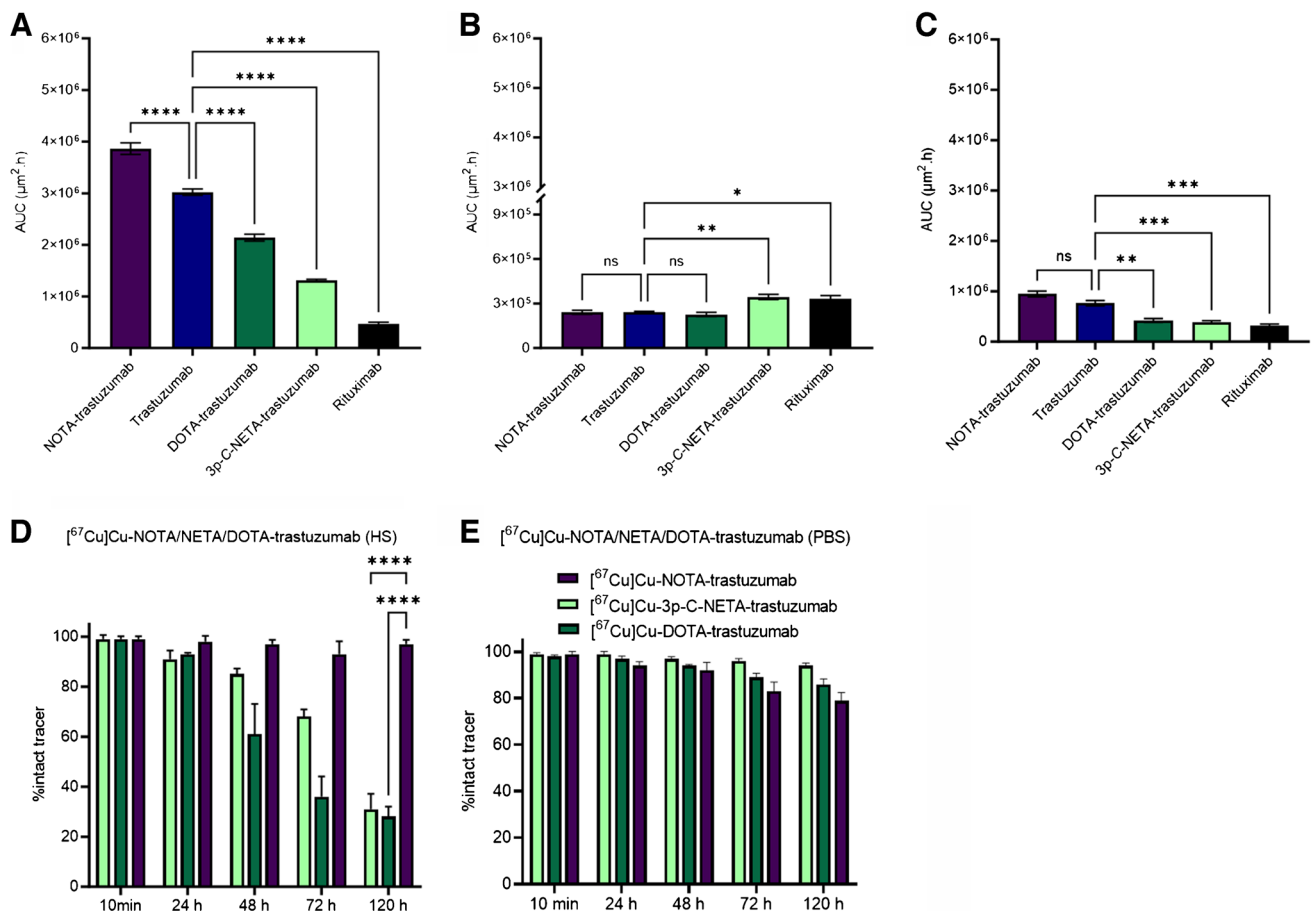
Fig. 1 Internalization and in vitro stability of antibody, immunoconjugates and RICs. Internalization of NOTA-trastuzumab, trastuzumab, DOTA-trastuzumab, 3p-*C*-NETA-trastuzumab, and control IgG (rituximab) in HER2-positive BT-474 (**A**), JIMT-1 (**B**) and MCF-7 (**C**) cells after 48 h incubation (both experiments were done in triplicates, $n = 3$). The extent of internalization was quantified using the area under the internalization-time curve (AUC) plotted using GraphPad Prism Version 9. Statistical significance of the extent of internalization of different treatments compared with naked trastuzumab was analyzed using a one-way ANOVA test with statistical significance of *$p = 0.0162$, **$p = 0.007$ (JIMT-1), **$p = 0.0022$ (MCF-7), ***$p = 0.001$, ****$p < 0.0001$ and ns (non-significant). Both BT-474 and MCF-7 had similar trends of internalization:NOTA-trastuzumab > trastuzumab > DOTA-trastuzumab > 3p-*C*-NETA-trastuzumab. (**D**) and (**E**) In vitro stability of [^{67}Cu]Cu-NOTA-trastuzumab, [^{67}Cu]Cu-3p-*C*-NETA-trastuzumab and [^{67}Cu]Cu-DOTA-trastuzumab in HS and PBS, respectively

further studies because of its stability in HS and PBS, and highest internalization rates.

Flow cytometry

Flow cytometry was used to determine the in vitro binding of trastuzumab and NOTA-trastuzumab in BT-474 (high HER2 expression), JIMT-1 (medium HER2 expression) and MCF-7 (low HER2 expression) cell lines. The in vitro binding of Cu^{stand}-NOTA-trastuzumab in BT-474 cells was also determined using flow cytometry. Conjugation of NOTA to trastuzumab decreased its binding to HER2-positive cells. The K_D of trastuzumab (8.2 ± 0.2 nM) was lower than that of NOTA-trastuzumab (26.5 ± 1.6 nM) in BT-474 cells. Similarly, trends were observed with JIMT-1 and MCF-7 cells (Fig. 2A, B, and C) (Supplementary Fig. S3A). There was no significance difference between the binding of NOTA-trastuzumab ($K_D = 19.1 \pm 0.4$ nM) and non-radioactive copper-labeled trastuzumab, Cu^{stand}-NOTA-trastuzumab ($K_D = 19.5 \pm 0.5$ nM in BT-474 cells ($p = 0.9852$) (Supplementary Fig. S3B).

Determination of chelator-to-antibody ratio, Radioligand binding and immunoreactivity

Conjugation of *p*-SCN-Bn-NOTA to trastuzumab (15:1 molar excess) resulted in an average of 2.9 NOTAs per trastuzumab molecule by isotopic dilution method (Fig. 3A).

Saturation radioligand binding assay was studied in BT-474 cells where the K_D of $[^{67}Cu]Cu$-NOTA-trastuzumab

was 2.1 ± 0.4 nM (Fig. 3B) showing that labeling of NOTA-trastuzumab with $[^{67}Cu]CuCl_2$ did not affect its binding characteristics.

The immunoreactive fraction of $[^{67}Cu]Cu$-NOTA-trastuzumab in BT-474 cells was determined to be $69.3 \pm 0.9\%$ (Fig. 3C).

Pharmacokinetics and radiation dosimetry

$[^{67}Cu]Cu$-NOTA-trastuzumab showed a bi-phasic half-life ($t_{1/2}$) with a fast distribution $t_{1/2\alpha}$ of 1.8 ± 0.8 h and a slow elimination $t_{1/2\beta}$ of 177.3 ± 24.6 h. The volume of distribution of the central compartment (V_1) was 1 ± 0.05 mL, and the volume of distribution at steady state (V_{ss}) was 2.02 ± 0.1 mL. The area under the blood concentration-time curve from 0 to 120 h was $12,441.5 \pm 1052.2\%$ IA.h/mL, and the systemic clearance was 0.008 ± 0.00073 mL/h (Fig. 4 and Table 1).

The greatest accumulation of radioactivity in healthy female Balb/c mice was found in blood ($25.1 \pm 1.5\%$ IA/g) with lower uptake in normal tissues such as the kidneys ($8.6 \pm 0.8\%$ IA/g), spleen ($9.8 \pm 1\%$ IA/g), lung ($9.6 \pm 0.4\%$ IA/g) and liver ($9.1 \pm 0.9\%$ IA/g) at 168 h p.i of $[^{67}Cu]Cu$-NOTA-trastuzumab (Supplementary Fig. S4A). The uptake and elimination of $[^{67}Cu]Cu$-NOTA-trastuzumab from normal tissues in mice was used to project the radiation absorbed doses in human female adults (Table 2). Human organ dosimetry estimates of $[^{67}Cu]Cu$-NOTA-trastuzumab shows the organ receiving the highest dose
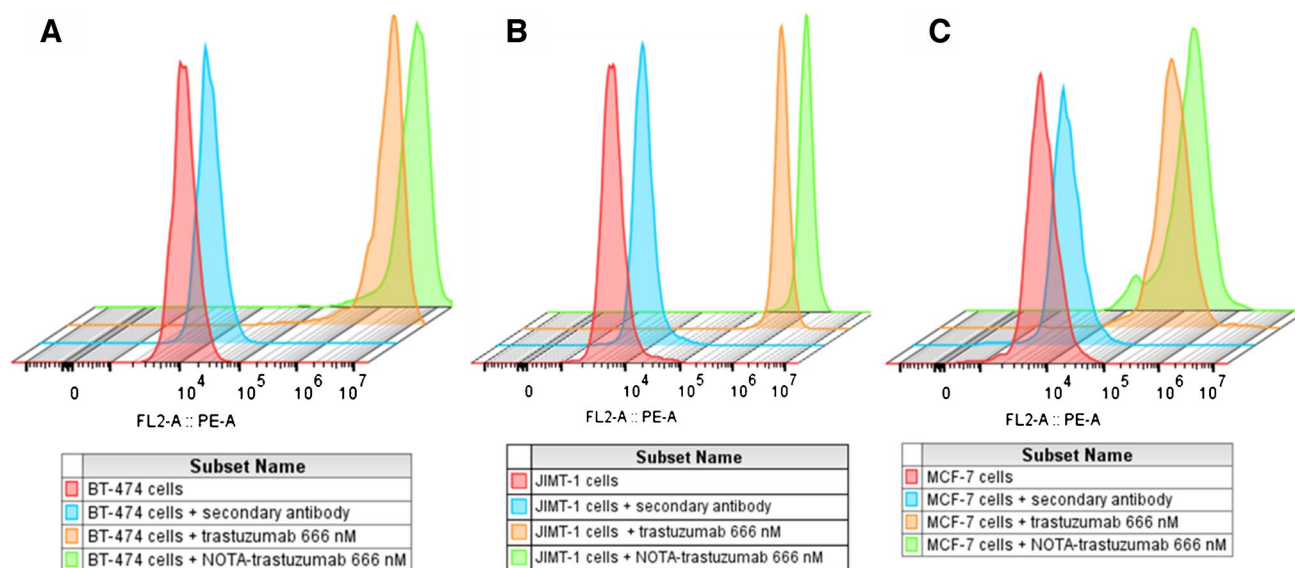

Fig. 2 Flow cytometry binding of immunoconjugates in HER2-positive cells. Three-dimensional flow cytometry histograms of cells alone, cells with secondary antibody (goat anti-human IgG Fc), trastuzumab and NOTA-trastuzumab. Binding was dependent on HER2 expression with the highest binding observed with BT-474 (**A**), followed by JIMT-1 (**B**) and MCF-7 (**C**) cells. These experiments were performed in triplicates ($n = 3$)
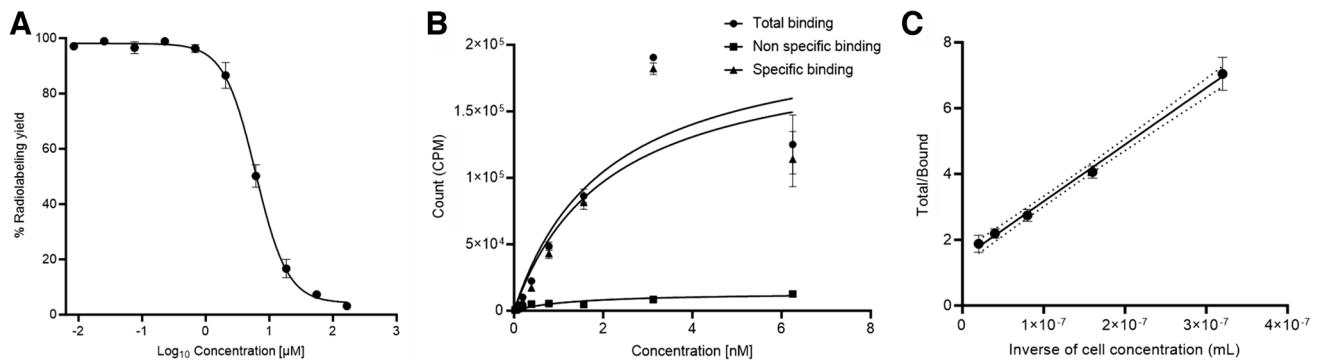
Fig. 3 Quality control (chelator-to-antibody ratio, radioligand binding assay and immunoreactive fraction) of radioimmunoconjugates. **A** Isotopic dilution method to determine the average number of NOTA that was conjugated to trastuzumab. Copper II Chloride ($CuCl_2$) was used as standard. **B** Radioligand binding assay of [^{67}Cu]Cu-NOTA-trastuzumab in BT-474 cells. Naked trastuzumab was used at 100 mol excess to saturate HER2 receptors prior to the addition of the labeled sample (non-specific binding). **C** Immunoreactive fraction of [^{67}Cu]Cu-NOTA-trastuzumab in BT-474 cells. Experiments were performed in triplicates ($n = 3$)
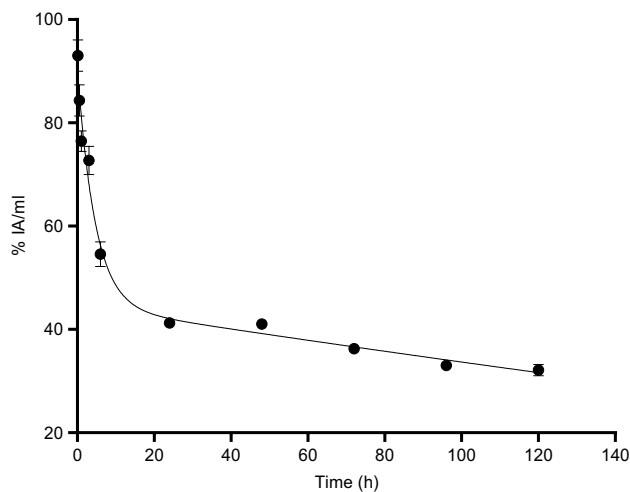
Fig. 4 Pharmacokinetics of [^{67}Cu]Cu-NOTA-trastuzumab in healthy female Balb/c mice ($n = 4$) showing a bi-phasic half-life ($t_{1/2}$) with fast distribution $t_{1/2\alpha}$ 1.8 ± 0.8 h and slow elimination $t_{1/2\beta}$ of 177.3 ± 24.6 h phases

Table 1 Pharmacokinetics parameters (mean ± SEM) of [^{67}Cu]Cu-NOTA-trastuzumab in healthy female Balb/c mice ($n = 4$)

PK parameters	Mean ± SEM
AUC (% IA.h/mL)	12,441.5 ± 1052.2
$t_{1/2\beta}$ (h)	177.3 ± 24.6
$V_1(V_c)$ (mL)	1 ± 0.05
V_{ss} (mL)	2.02 ± 0.1
CL (mL/h)	0.00818 ± 0.00073
$t_{1/2\alpha}$ (h)	1.8 ± 0.8

Table 2 Projected human absorbed doses (mSv/MBq) of [^{67}Cu]Cu-NOTA-trastuzumab using biodistribution data of healthy Balb/c mice ($n = 4$)

| Organs	mSv/MBq female
Adrenals	3.18E-02
Brain	2.51E-02
Breast	5.75E-03
Esophagus	2.28E-02
Eyes	1.26E-03
Gall bladder	2.22E-02
Left colon	9.05E-03
Small intestine	1.15E-01
Stomach	4.16E-02
Right colon	4.95E-02
Rectum	1.32E-03
Heart wall	2.81E-01
Kidneys	3.54E-01
Liver	3.51E-01
Lungs	4.09E-01
Ovaries	2.53E-03
Pancreas	1.26E-01
Salivary glands	1.78E-03
Red marrow	1.04E-02
Spleen	3.90E-01
Thymus	1.99E-02
Thyroid	7.93E-03
Bladder	1.12E-03
Uterus	2.62E-03
Total body	2.51E-02
Effective dose	1.71E-02

are the lungs > spleen > kidneys > liver, and total whole-body dose estimate of 2.51×10^{-2} mSv/MBq.

The mice bearing JIMT-1 xenograft had high radioactivity uptake in the tumor ($33.9 \pm 5.5\%$ IA/g) with low uptake in normal tissues such as the liver ($6.5 \pm 0.5\%$ IA/g), lungs ($6.0 \pm 0.7\%$ IA/g), spleen ($5.6 \pm 0.4\%$ IA/g) at 120 h p.i of [^{67}Cu]Cu-NOTA-trastuzumab (Supplementary Fig. S4B). Dosimetry in female athymic Balb/c nude mice bearing JIMT-1 tumors showed high doses in spleen > liver > lungs > kidneys (Supplementary Table S1).

ImmunoSPECT/CT imaging and biodistribution

ImmunoSPECT/CT imaging using [^{67}Cu]Cu-NOTA-trastuzumab in BT-474/MCF-7 (high/low HER2 expression) (Fig. 5A) and in JIMT-1 (medium HER2 expression) (Fig. 5B) tumor-bearing mice were done at 24, 48, and 120 h post injection (p.i.). Tumor uptake was dependent on HER2 density with the highest uptake in BT-474 and JIMT-1. Biodistribution studies showed tumor uptake of [^{67}Cu]Cu-NOTA-trastuzumab in female athymic Balb/c nude mice xenografts increased slightly from $32.3 \pm 1.7\%$ IA/g at 24 h p.i. to $33.1 \pm 10.6\%$ IA/g at 120 h p.i. for BT-474 ($p = 0.9996$), increased significantly from $9.2 \pm 1.2\%$ IA/g at 24 h p.i. to $33.9 \pm 5.5\%$ IA/g at 120 h p.i for JIMT-1 ($p = 0.0230$), but decreased slightly from $15.2 \pm 3\%$ IA/g at 24 h p.i. to $14.6 \pm 2.7\%$ IA/g at 120 h p.i. for MCF-7 ($p = 0.9999$). Uptake of [^{67}Cu]Cu-NOTA-trastuzumab in BT-474 tumor was more than two fold greater than that of MCF-7 at 24 h and 120 h p.i. There was a high uptake in blood followed by the spleen (blood: $12.8 \pm 2.5\%$ IA/g; spleen: $8.5 \pm 2.6\%$ IA/g) of the labeled antibody at 24 h p.i in BT-474/MCF-7 mice xenografts. This uptake later decreased to $5.6 \pm 2.4\%$ IA/g (blood) and $3.2 \pm 0.7\%$ IA/g (spleen) at 120 h p.i. (Fig. 5C). Tumor to blood ratio (T/B) for BT-474, JIMT-1 and MCF-7 increased from 2.5 to 5.9, 1.5 to 2.0
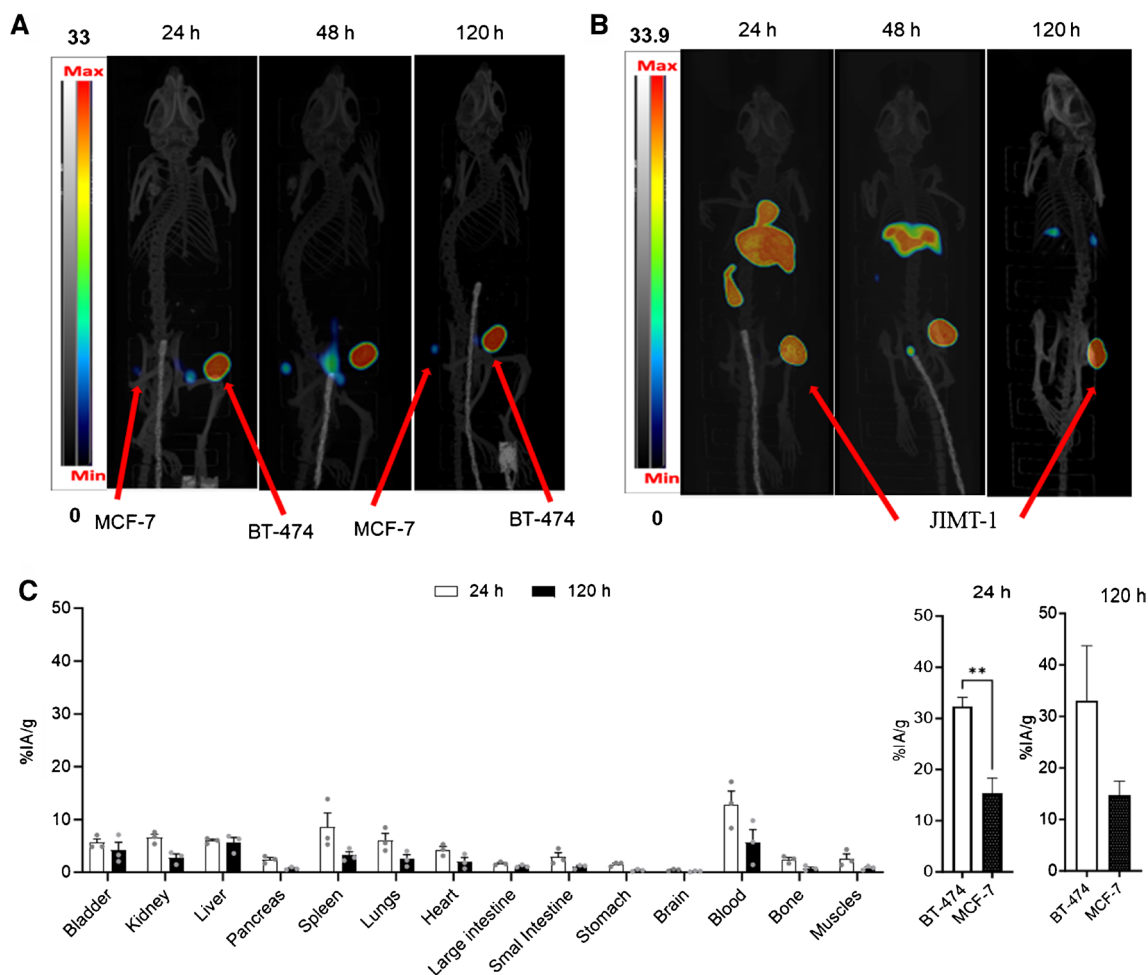
Fig. 5 MicroSPECT/CT imaging and biodistribution of [^{67}Cu]Cu-NOTA-trastuzumab. Molecular imaging of HER2-positive BC xenografts (MCF-7 (left flank) and BT-474 (right flank)) (**A**) and JIMT-1 (**B**) in female athymic Balb/c nude mice at 24, 48 and 120 h p.i. after a tail vein injection of 10-11 MBq of [^{67}Cu]Cu-NOTA-trastuzumab, and (**C**) Biodistribution of female athymic Balb/c nude mice ($n = 3$) bearing BT-474 and MCF-7 xenografts after a tail vein injection of [^{67}Cu]Cu-NOTA-trastuzumab

and 1.2 to 2.6 respectively, at 24 h and 120 h p.i. Similar trends were observed for tumor-to-muscle, tumor-to-lungs, and tumor-to-liver ratios in all xenografts (Supplementary Fig. S4C).

Radioimmunotherapy

[67Cu]Cu-NOTA-trastuzumab was very effective against HER2-positive BT-474 and JIMT-1 xenografts. Six of eight (6/8) mice bearing BT-474 xenograft treated with [67Cu]Cu-NOTA-trastuzumab had complete remission (CR) after 54 days of treatment compared with 2/6 CRs in the trastuzumab group. The average tumor sizes in BT-474 mice after day 28 of treatment were 155.5 ± 107.7 mm^3 (trastuzumab group), 300.7 ± 89.2 mm^3 (saline) and 9.5 ± 6 mm^3 ([67Cu]Cu-NOTA-trastuzumab) (Fig. 6).

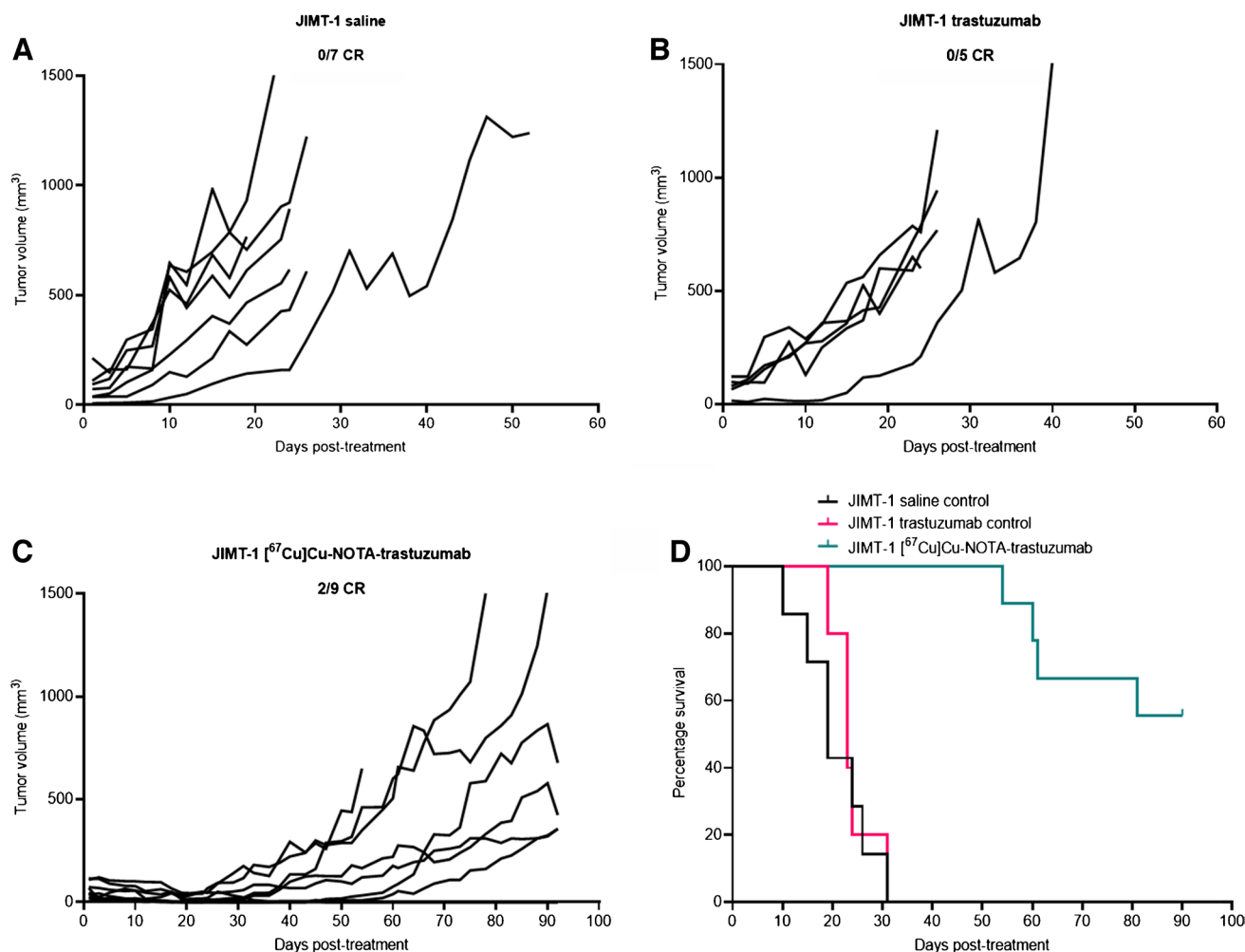JIMT-1 tumor-bearing mice treated using [67Cu]Cu-NOTA-trastuzumab experienced a decrease in tumor volume from the first day of treatment to day 20 post-treatment. The average tumor size of JIMT-1 tumors after day 20 of treatment was 416.8 ± 76.4 mm^3 (trastuzumab), 610.2 ± 94.8 mm3 (saline) and 10.2 ± 4.5 mm^3 ([67Cu]Cu-NOTA-trastuzumab). After day 54 of treatment, 2/9 mice bearing JIMT-1 tumors treated with [67Cu]Cu-NOTA-trastuzumab had CR while 7/9 mice showed partial response, and there were no CRs in trastuzumab or saline groups (Fig. 7).

[67Cu]Cu-NOTA-trastuzumab was more effective than trastuzumab in both BT-474 xenografts (78% vs 54% TGI after 28 days) and JIMT-1 xenografts (90% vs 23% TGI after 19 days), respectively (Supplementary Fig. S5B showing average tumor volumes in mm^3). [67Cu]Cu-NOTA-trastuzumab and trastuzumab were well tolerated than [177Lu]Lu-DOTA-trastuzumab as evident in the increase in body weights in all treated groups (Supplementary Fig. S5A and C).
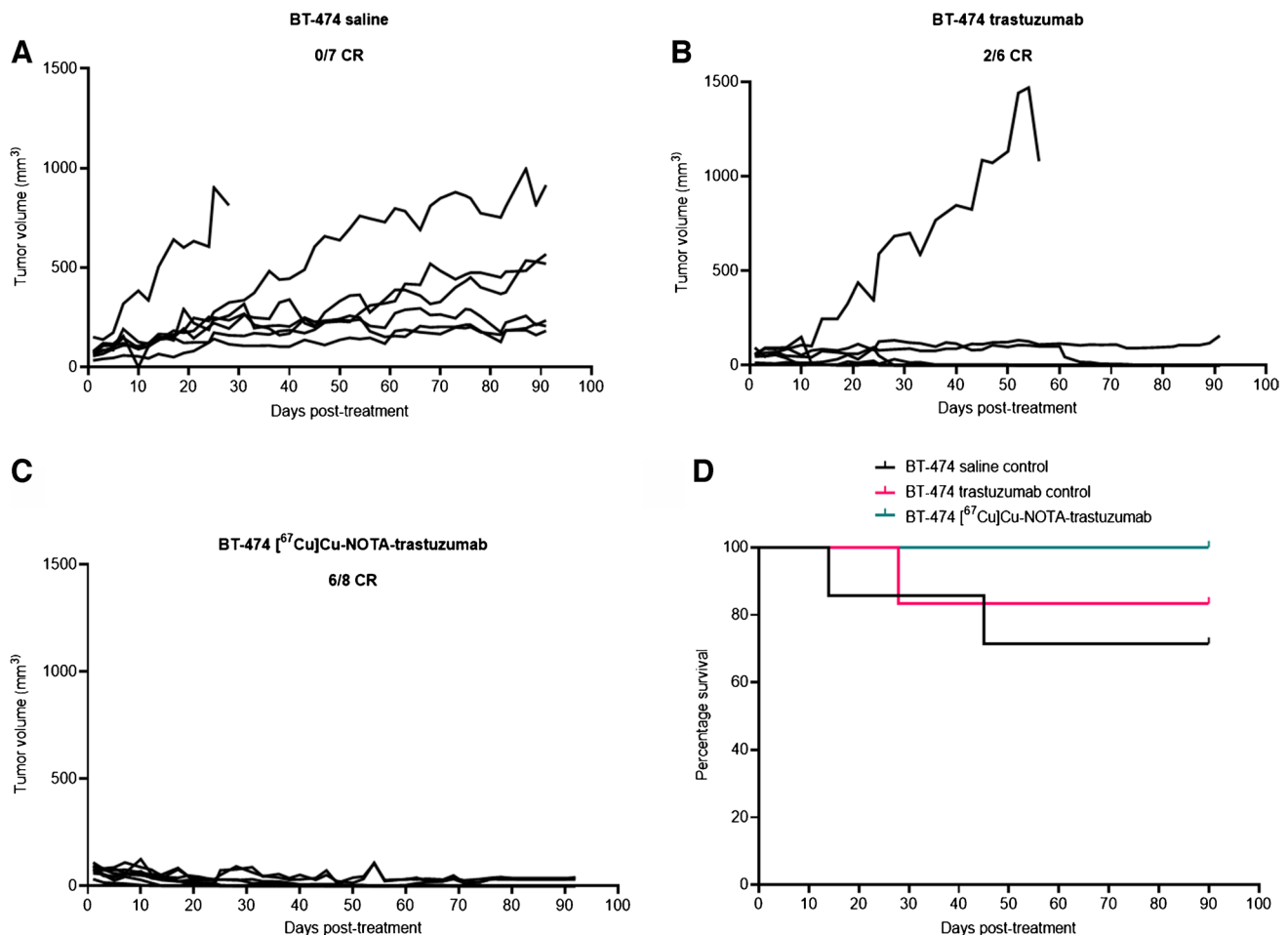
Fig. 6 Efficacy of [67Cu]Cu-NOTA-trastuzumab against HER2-positive BT-474 xenograft. BT-474 tumor bearing athymic Balb/c nude mice (n=6-8/group) were not treated (**A**) or treated using a single dose of trastuzumab (**B**) or with a single dose of ~ 16.8 MBq of [67Cu]Cu-NOTA-trastuzumab (**C**), and (**D**) is Kaplan Meier survival fractions of the treated and non-treated groups. CR: Complete remission

Fig. 7 Efficacy of [^{67}Cu]Cu-NOTA-trastuzumab against HER2-positive JIMT-1 xenografts. JIMT-1 tumor bearing athymic Balb/c nude mice ($n = 5$-9/group) were not treated (**A**) or treated using a single dose of trastuzumab (**B**) or with a single dose of ~16.8 MBq of [^{67}Cu]Cu-NOTA-trastuzumab (**C**), and (**D**) is Kaplan Meier survival fractions of the treated and non-treated groups. CR: Complete remission. Six of eight JIMT-1 tumor-bearing mice treated using [^{177}Lu] Lu-DOTA-trastuzumab experienced a decrease in tumor volume from the first day of treatment to day 13 post-treatment. The average tumor size of JIMT-1 tumors after day 13 of treatment was 70.8 ± 20.8 mm^3. From day 14 to 22 of treatment, 6/8 mice bearing JIMT-1 tumors treated with [^{177}Lu]Lu-DOTA-trastuzumab experienced more than 20% weight loss indicative of systemic toxicity and had to be euthanized (Supplementary Fig. S5C)

Discussion

HER2-positive BC is characterized by poor prognosis, disease progression, aggressiveness, and low overall survival rates, hence an "incompletely resolved" health issue [3, 19]. The theranostic approach involving radiolabeled imaging and a therapeutic agent has the potential to improve cancer management and resolve this health issue. Trastuzumab is the most widely used anti-HER2 monoclonal antibody (mAb) therapeutic but its benefits in patients when used as a naked antibody is limited [38]. Since the late '80 s, copper-67 has been suggested as an effective theranostic radioisotope for radioimmunotherapy of cancers when Shrikant et al. demonstrated the efficacy of ^{67}Cu-labeled mAb

Lym-1 against B cell lymphoma in RAJI mice xenografts [39]. Compared with ^{67}Cu, other widely used beta-emitters such as ^{177}Lu, ^{131}I, and ^{90}Y do not have/have less than ideal branching ratios for their gamma energies for imaging purposes for a true theranostic approach [40]. To the best of our knowledge, [^{67}Cu]Cu-trastuzumab has not been evaluated as an anti-HER2 theranostic. Here, we have described the development of [^{67}Cu]Cu-trastuzumab starting with the selection of the most stable chelator for [^{67}Cu]CuCl$_2$.

P-SCN-Bn-NOTA, 3p-*C*-NETA-NCS, and *p*-SCN-Bn-DOTA are potential bifunctional chelators (BFCs) in terms of in vitro stability and labeling kinetics for ^{177}Lu, and ^{90}Y [3, 41]. We conjugated trastuzumab with these three BFCs and labeled with ^{67}Cu followed by evaluation of their in vitro

stability and antibody internalization rates. Conjugation of trastuzumab with these BFCs yielded > 98% pure immuno-conjugates (NOTA-trastuzumab, 3p-*C*-NETA-trastuzumab, and DOTA-trastuzumab) confirmed by SEC-HPLC and the bioanalyzer. For therapeutic purposes, an antibody needs to bind to the cell surface receptor as well as internalize into the cell [42]. Highest internalization was observed with NOTA-trastuzumab in both BT-474 and MCF-7 BC cell lines (Fig. 1A and C). This could be due to a desirable hydrophilicity/lipophilicity ratio and physiological charge, enabling the antibody to bind with increasing internalization. Compared with MCF-7, JIMT-1 showed lower extent of internalization despite having higher HER2 density (Fig. 1B). Nagy et al. showed that masking (and hence poor internalization rate) of HER2 in JIMT-1 is the primary reason of resistance of the cells to anti-HER2 targeted monoclonal antibody and ADC therapeutics [43]. Compared with [67Cu]Cu-3p-*C*-NETA-trastuzumab and [67Cu]Cu-DOTA-trastuzumab, [67Cu]Cu-NOTA-trastuzumab was more stable in HS (Fig. 1D and E). Similar results were obtained in a previous study comparing [64Cu]Cu-NOTA-trastuzumab and [64Cu]Cu-DOTA-trastuzumab in vitro and in vivo [3, 44, 45]. Priya et al. showed that [177Lu]Lu-trastuzumab was only stable for 12 h after labelling which is far less than what we obtained for [67Cu]Cu-NOTA-trastuzumab [11]. Despite the excellent stability of [67Cu]Cu-3p-*C*-NETA-trastuzumab in PBS, it was less stable in HS, confirming previous result where [67Cu]CuCl$_2$ was labeled using 3p-*C*-NETA BFC [41]. Hence [67Cu]Cu-NOTA-trastuzumab was chosen to evaluate its theranostic potential against HER2-positive BC models.

As expected, conjugation of *p*-SCN-Bn-NOTA to trastuzumab decreased the binding of trastuzumab to HER2 (Fig. 2 and Supplementary Fig. S3A), and this was observed in BT-474, JIMT-1 and MCF-7 cells with respectively high, medium, and low HER2 expression. The average number of NOTA chelator per trastuzumab molecule was determined to be 2.9 using isotopic dilution method. Hao et al., obtained a NOTA: pertuzumab ratio of 1.9 using a 20-fold molar excess of the chelator during conjugation [24], while Lam et al. obtained a substitution level of 4.1 NOTA/F(ab')$_2$ after conjugation of the fragment with ten fold molar excess of NOTA [46]. Binding of both non-radioactive (Cu^{stand}-NOTA-trastuzumab) and radiolabeled [67Cu]Cu-NOTA-trastuzumab was not different from the NOTA-trastuzumab or naked antibody, respectively, as confirmed by their K_D, the saturation binding (2.1 ± 0.4 nM) and immunoreactive fraction (69.3 ± 0.9%) (Fig. 3B and C, Supplementary Fig. S3B). Similarly, [177Lu]Lu-DOTA-trastuzumab had an immunoreactivity of 72–77% against HER2 protein [11].

Pharmacokinetics is one of the critical attributes that affects the therapeutic index of a therapeutic agent. [67Cu]Cu-NOTA-trastuzumab showed good pharmacokinetics (Table 1 and Fig. 4) with a terminal elimination half-life (t$_{1/2β}$) of 177.3 ± 24.6 h. The t$_{1/2β}$ of [64Cu]Cu-NOTA-trastuzumab in healthy female mice without tumors 72 h p.i. was 190 ± 40.2 h [3].

[67Cu]Cu-NOTA-trastuzumab delivered very low dose to all healthy organs due to its favorable clearance rates from all healthy tissues. It is worth nothing that trastuzumab does not cross react with murine HER2 with the potential consequence of underestimating human doses using murine biodistribution data. The highest organ dose was observed for the liver, kidneys, lungs, and spleen. By comparison, widely investigated anti-HER2 RIC such as [177Lu]Lu-DTPA-trastuzumab had liver and spleen doses of 1.72 Gy/MBq (1720 mSv/MBq) and 1.6 Gy/MBq (1600 mSv/MBq), respectively which is several folds higher than [67Cu]Cu-NOTA-trastuzumab [47]. In the current study, the lung was one of the organ that received the highest dose of [67Cu]Cu-NOTA-trastuzumab, consistent with the biodistribution data that showed persistent high uptake in healthy Balb/c mice. The observed high lung uptake has been reported by other authors for [177Lu]Lu-labeled trastuzumab [48, 49]. The potential consequence of this is the risk of damage to lung tissue in patients. Interstitial lung injury (ILD) has been reported in clinical studies for patients receiving trastuzumab deruxtecan an anti-HER2 antibody drug conjugate [50] which is linked to the high lung uptake of the potent agent. Therefore, patients receiving potent radioimmunoconjugates of trastuzumab should be monitored for ILD.

Due to the better branching ratios of its gamma emissions, immunoSPECT using ^{67}Cu would theoretically result in images of better diagnostic quality compared with ^{177}Lu. The specific gamma-ray dose constant of ^{67}Cu (2.363×10^{-5} (mSv/h)/MBq) is three times higher than that of ^{177}Lu (7.636×10^{-6} (mSv/h)/MBq) [51]. BT-474, JIMT-1 and MCF-7 tumors in female athymic Balb/c nude mice were well delineated with [67Cu]Cu-NOTA-trastuzumab SPECT with the highest uptake obtained after 5 days p.i. for BT-474 and MCF-7. As expected, MCF-7 with low HER2 expression has significantly lower tumor 14.6 ± 2.7% IA/g at 120 h p.i. (Fig. 5), confirming the specificity of the radioimmunoconjugate.

A single dose of [67Cu]Cu-NOTA-trastuzumab was very effective against BT-474 (trastuzumab sensitive) tumor-bearing mice and JIMT-1 (trastuzumab-resistant) tumor-bearing mice. The percentage tumor growth inhibition (TGI) in BT-474 xenografts was 78% and 54% after 28 days for [67Cu]Cu-NOTA-trastuzumab and trastuzumab as compared to the control group (saline) respectively. The median survival of [67Cu]Cu-NOTA-trastuzumab was prolonged to > 90 days compared with trastuzumab (77 days) and saline (72 days) groups for BT-474 xenograft (Fig. 6). We found that a single dose of ~ 16.8 MBq of [67Cu]Cu-NOTA-trastuzumab led to a high BT-474 tumor inhibition and prolonged the survival compared with unlabeled trastuzumab and control

group, with 6/8 complete CRs. Better tumor inhibition was observed with JIMT-1 xenografts after a single injection of ~ 16.8 MBq of [67Cu]Cu-NOTA-trastuzumab. After 19 days post treatment, [67Cu]Cu-NOTA-trastuzumab (90%) was more effective than trastuzumab (23%) in both JIMT-1 xenografts and the mean survival of [67Cu]Cu-NOTA-trastuzumab, trastuzumab and saline groups were 78, 24, and 20 days. These results were better than those obtained by Rasaneh et al. where the percentage tumor inhibition in HER2-positive tumors were 81% after a longer period of 42 days of treatment with [177Lu]Lu-DOTA-trastuzumab [52]. We attempted to compare the effectiveness of [67Cu]Cu-NOTA-trastuzumab with [177Lu]Lu-DOTA-trastuzumab at similar dose. JIMT-1 xenografts that received a single dose of ~ 16.8 MBq of [177Lu]Lu-DOTA-trastuzumab was not well tolerated probably due to the high activity administered as seen by their weight loss (Supplementary Fig. S5C). About 7.4 MBq/30 µg of [177Lu]Lu-DOTA-trastuzumab was injected in tumor bearing mice and seemed well tolerated [52].

Conclusion

To the best of our knowledge, our work is the first to compare the suitability of [67Cu]Cu-NOTA-trastuzumab, [67Cu]Cu-3p-*C*-NETA-trastuzumab and [67Cu]Cu-DOTA-trastuzumab as anti-HER2 theranostics. [67Cu]Cu-NOTA-trastuzumab was the most stable radiocomplex. The exciting immunoSPECT imaging of [67Cu]Cu-NOTA-trastuzumab even at 120 h p.i. shows that it has great potential for imaging. Administration of a single dose of ~ 16.8 MBq of [67Cu]Cu-NOTA-trastuzumab to BT-474 and JIMT-1 tumor bearing athymic Balb/c nude mice resulted in high anti-tumor efficacy and tolerance. [67Cu]Cu-NOTA-trastuzumab is therefore a promising theranostic agent against HER2-positive BC and necessitates clinical investigation.

Declarations

References

1. Chhikara BS, Parang K. Global Cancer Statistics 2022: the trends projection analysis. Chem Biol Lett. 2022;10:451.

2. Latta EK, Tjan S, Parkes RK, O'Malley FP. The role of HER2/neu overexpression/amplification in the progression of ductal carcinoma in situ to invasive carcinoma of the breast. Mod Pathol. 2002;15:1318–25. https://doi.org/10.1097/01.mp.0000038462.62634.b1.

3. Woo S-K, Jang SJ, Seo M-J, Park JH, Kim BS, Kim EJ, et al. Development of 64Cu-NOTA-Trastuzumab for HER2 targeting: A radiopharmaceutical with improved pharmacokinetics for human studies. J Nucl Med. 2019;60:26–33. https://doi.org/10.2967/jnumed.118.210294.

4. Swain SM, Shastry M, Hamilton E. Targeting HER2-positive breast cancer: advances and future directions. Nat Rev Drug Discovery. 2023;22:101–26. https://doi.org/10.1038/s41573-022-00579-0.

5. Altunay B, Morgenroth A, Beheshti M, Vogg A, Wong NCL, Ting HH, et al. HER2-directed antibodies, affibodies and nanobodies as drug-delivery vehicles in breast cancer with a specific focus on radioimmunotherapy and radioimmunoimaging. Eur J Nucl Med Mol Imaging. 2021;48:1371–89. https://doi.org/10.1007/s00259-020-05094-1.

6. Gote V, Nookala AR, Bolla PK, Pal D. Drug Resistance in Metastatic Breast Cancer: Tumor Targeted Nanomedicine to the Rescue. Int J Mol Sci. 2021;22:4673. https://doi.org/10.3390/ijms22094673.

7. Choong GM, Cullen GD, O'Sullivan CC. Evolving standards of care and new challenges in the management of HER2-positive breast cancer. CA A Cancer J Clin. 2020;70:355–74. https://doi.org/10.3322/caac.21634.

8. Menon SR, Mitra A, Chakraborty A, Tawate M, Sahu S, Rakshit S, et al. Clinical dose preparation of [177Lu]Lu-DOTA-Pertuzumab using medium specific activity [177Lu]LuCl3 for radioimmunotherapy of breast and epithelial ovarian cancers, with HER2 receptor overexpression. Cancer Biother Radiopharm. 2022;37:384–402. https://doi.org/10.1089/cbr.2021.0230.

9. Rondon A, Rouanet J, Degoul F. Radioimmunotherapy in oncology: Overview of the last decade clinical trials. Cancers. 2021;13:5570. https://doi.org/10.3390/cancers13215570.

10. Meredith R, Torgue J, Shen S, Fisher DR, Banaga E, Bunch P, et al. Dose escalation and dosimetry of first-in-human α radioimmunotherapy with 212Pb-TCMC-trastuzumab. J Nucl Med. 2014;55:1636–42. https://doi.org/10.2967/jnumed.114.143842.

11. Bhusari P, Vatsa R, Singh G, Parmar M, Bal A, Dhawan DK, et al. Development of Lu-177-trastuzumab for radioimmunotherapy of HER2 expressing breast cancer and its feasibility assessment in breast cancer patients. Int J Cancer. 2017;140:938–47. https://doi.org/10.1002/ijc.30500.

12. Liu Y, Xu T, Vorobyeva A, Loftenius A, Bodenko V, Orlova A, et al. Radionuclide Therapy of HER2-Expressing Xenografts Using [(177)Lu]Lu-ABY-027 Affibody Molecule Alone and in Combination with Trastuzumab. Cancers (Basel). 2023;15. https://doi.org/10.3390/cancers15092409.

13. Orlova A, Jonsson A, Rosik D, Lundqvist H, Lindborg M, Abrahmsen L, et al. Site-specific radiometal labeling and improved biodistribution using ABY-027, a novel HER2-targeting affibody molecule-albumin-binding domain fusion protein. J Nucl Med. 2013;54:961–8. https://doi.org/10.2967/jnumed.112.110700.

14. Kvassheim M, Revheim MR, Stokke C. Quantitative SPECT/CT imaging of lead-212: a phantom study. EJNMMI Phys. 2022;9:52. https://doi.org/10.1186/s40658-022-00481-z.

15. Abbas N, Bruland OS, Brevik EM, Dahle J. Preclinical evaluation of 227Th-labeled and 177Lu-labeled trastuzumab in mice with HER-2-positive ovarian cancer xenografts. Nucl Med Commun. 2012;33:838–47. https://doi.org/10.1097/MNM.0b013e328354df7c.

16. Abbas N, Heyerdahl H, Bruland OS, Borrebaek J, Nesland J, Dahle J. Experimental alpha-particle radioimmunotherapy of breast cancer using 227Th-labeled p-benzyl-DOTA-trastuzumab. EJNMMI Res. 2011;1:18. https://doi.org/10.1186/2191-219X-1-18.

17. Abou DS, Longtine M, Fears A, Benabdallah N, Unnerstall R, Johnston H, et al. Evaluation of Candidate Theranostics for 227Th/89Zr Paired Radioimmunotherapy of Lymphoma. J Nucl Med. 2023;64:1062–8. https://doi.org/10.2967/jnumed.122.264979.

18. Bodei L, Herrmann K, Schöder H, Scott AM, Lewis JS. Radiotheranostics in oncology: current challenges and emerging opportunities. Nat Rev Clin Oncol. 2022;19:534–50. https://doi.org/10.1038/s41571-022-00652-y.

19. Vahidfar N, Aghanejad A, Ahmadzadehfar H, Farzanehfar S, Eppard E. Theranostic advances in breast cancer in nuclear medicine. Int J Mol Sci. 2021;22:4597. https://doi.org/10.3390/ijms22094597.

20. Reubi JC, Schar JC, Waser B, Wenger S, Heppeler A, Schmitt JS, et al. Affinity profiles for human somatostatin receptor subtypes SST1-SST5 of somatostatin radiotracers selected for scintigraphic and radiotherapeutic use. Eur J Nucl Med. 2000;27:273–82. https://doi.org/10.1007/s002590050034.

21. Fani M, Nicolas GP, Wild D. Somatostatin receptor antagonists for imaging and therapy. J Nucl Med. 2017;58:61S-S66. https://doi.org/10.2967/jnumed.116.186783.

22. Mou L, Martini P, Pupillo G, Cieszykowska I, Cutler CS, Mikolajczak R. (67)Cu production capabilities: A mini review. Molecules. 2022;27. https://doi.org/10.3390/molecules27051501.

23. Lee JY, Chae JH, Hur MG, Yang SD, Kong YB, Lee J, et al. Theragnostic (64)Cu/(67)Cu radioisotopes production with RFT-30 cyclotron. Front Med (Lausanne). 2022;9:889640. https://doi.org/10.3389/fmed.2022.889640.

24. Hao G, Mastren T, Silvers W, Hassan G, Oz OK, Sun X. Copper-67 radioimmunotheranostics for simultaneous immunotherapy and immuno-SPECT. Sci Rep. 2021;11:3622. https://doi.org/10.1038/s41598-021-82812-1.

25. Cullinane C, Jeffery CM, Roselt PD, van Dam EM, Jackson S, Kuan K, et al. Peptide receptor radionuclide therapy with (67)Cu-CuSarTATE Is highly efficacious against a somatostatin-positive neuroendocrine tumor model. J Nucl Med. 2020;61:1800–5. https://doi.org/10.2967/jnumed.120.243543.

26. Simon M, Jorgensen JT, Khare HA, Christensen C, Nielsen CH, Kjaer A. Combination of [(177)Lu]Lu-DOTA-TATE targeted radionuclide therapy and photothermal therapy as a promising approach for cancer treatment: In vivo studies in a human xenograft mouse model. Pharmaceutics. 2022;14. https://doi.org/10.3390/pharmaceutics14061284.

27. Loft M, Carlsen EA, Johnbeck CB, Johannesen HH, Binderup T, Pfeifer A, et al. (64)Cu-DOTATATE PET in patients with neuroendocrine neoplasms: prospective, head-to-head comparison of imaging at 1 hour and 3 hours after injection. J Nucl Med. 2021;62:73–80. https://doi.org/10.2967/jnumed.120.244509.

28. Liang Y, Besch-Williford C, Hyder SM. PRIMA-1 inhibits growth of breast cancer cells by re-activating mutant p53 protein. Int J Oncol. 2009;35:1015–23. https://doi.org/10.3892/ijo_00000416.

29. Tomayko MM, Reynolds CP. Determination of subcutaneous tumor size in athymic (nude) mice. Cancer Chemother Pharmacol. 1989;24:148–54. https://doi.org/10.1007/bf00300234.

30. Hartimath SV, Alizadeh E, Solomon VR, Chekol R, Bernhard W, Hill W, et al. Preclinical evaluation of 111In-Labeled PEGylated maytansine nimotuzumab drug conjugates in EGFR-positive cancer models. J Nucl Med. 2019;60:1103–10. https://doi.org/10.2967/jnumed.118.220095.

31. Meares CF, McCall MJ, Reardan DT, Goodwin DA, Diamanti CI, McTigue M. Conjugation of antibodies with bifunctional chelating agents: Isothiocyanate and bromoacetamide reagents, methods of analysis, and subsequent addition of metal ions. Anal Biochem. 1984;142:68–78. https://doi.org/10.1016/0003-2697(84)90517-7.

32. Ketchemen JP, Babeker H, Tikum AF, Nambisan AK, Njotu FN, Nwangele E, et al. Biparatopic anti-HER2 drug radioconjugates as breast cancer theranostics. Br J Cancer. 2023. https://doi.org/10.1038/s41416-023-02272-4.

33. Tikum AF, Nambisan AK, Ketchemen JP, Babeker H, Khan MN, Torlakovic EE, et al. Simultaneous imaging and therapy using Epitope-Specific Anti-Epidermal Growth Factor Receptor (EGFR) antibody conjugates. Pharmaceutics. 2022;14:1917. https://doi.org/10.3390/pharmaceutics14091917.

34. Lindmo T, Boven E, Cuttitta F, Fedorko J, Bunn PA. Determination of the immunoreactive function of radiolabeled monoclonal antibodies by linear extrapolation to binding at infinite antigen excess. J Immunol Methods. 1984;72:77–89. https://doi.org/10.1016/0022-1759(84)90435-6.

35. Babeker H, Ketchemen JP, Annan Sudarsan A, Andrahennadi S, Tikum AF, Nambisan AK, et al. Engineering of a fully human anti-MUC-16 antibody and evaluation as a PET imaging agent. Pharmaceutics. 2022;14:2824. https://doi.org/10.3390/pharmaceutics14122824.

36. Kirschner AS, Ice RD, Beierwaltes WH. Radiation-dosimetry of I-131-19-Iodocholesterol - pitfalls of using tissue concentration data - reply. J Nucl Med. 1975;16:248–9.

37. Laforest R, Lapi SE, Oyama R, Bose R, Tabchy A, Marquez-Nostra BV, et al. [Zr-89]Trastuzumab: evaluation of radiation dosimetry, safety, and optimal imaging parameters in women with HER2-positive breast cancer. Mol Imag Biol. 2016;18:952–9. https://doi.org/10.1007/s11307-016-0951-z.

38. Slamon D, Eiermann W, Robert N, Pienkowski T, Martin M, Press M, et al. Adjuvant Trastuzumab in HER2-Positive Breast Cancer. N Engl J Med. 2011;365:1273–83. https://doi.org/10.1056/nejmoa0910383.

39. Shrikant VD, Sally JD, Claude FM, Michael JM, Gregory PA, Min KM, et al. Copper-67-labeled monoclonal antibody Lym-1, a potential radiopharmaceutical for cancer therapy: labeling and biodistribution in RAJI tumored mice. J Nucl Med. 1988;29:217.

40. Stokke C, Kvassheim M, Blakkisrud J. Radionuclides for targeted therapy: physical properties. Molecules. 2022;27:5429. https://doi.org/10.3390/molecules27175429.

41. Ahenkorah S, Murce E, Cawthorne C, Ketchemen JP, Deroose CM, Cardinaels T, et al. 3p-C-NETA: A versatile and effective chelator for development of Al¹⁸F-labeled and

therapeutic radiopharmaceuticals. Theranostics. 2022;12:5971–85. https://doi.org/10.7150/thno.75336.

42. Zhou Y, Marks JD. Discovery of internalizing antibodies to tumor antigens from phage libraries. Methods Enzymol. 2012;502:43–66. https://doi.org/10.1016/b978-0-12-416039-2.00003-3.

43. Nagy P, Friedlander E, Tanner M, Kapanen AI, Carraway KL, Isola J, et al. Decreased accessibility and lack of activation of ErbB2 in JIMT-1, a herceptin-resistant, MUC4-expressing breast cancer cell line. Cancer Res. 2005;65:473–82.

44. Guleria M, Das T, Amirdhanayagam J, Sarma HD, Dash A. Comparative evaluation of using NOTA and DOTA derivatives as bifunctional chelating agents in the preparation of (68)Ga-labeled porphyrin: impact on pharmacokinetics and tumor uptake in a mouse model. Cancer Biother Radiopharm. 2018;33:8–16. https://doi.org/10.1089/cbr.2017.2337.

45. Roosenburg S, Laverman P, Joosten L, Cooper MS, Kolenc-Peitl PK, Foster JM, et al. PET and SPECT imaging of a radiolabeled minigastrin analogue conjugated with DOTA, NOTA, and NODAGA and labeled with ^{64}Cu, ^{68}Ga, and [111]In. Mol Pharm. 2014;11:3930–7. https://doi.org/10.1021/mp500283k.

46. Lam K, Chan C, Reilly RM. Development and preclinical studies of 64Cu-NOTA-pertuzumab F(ab')2 for imaging changes in tumor HER2 expression associated with response to trastuzumab by PET/CT. mAbs. 2017;9:154–64. https://doi.org/10.1080/19420862.2016.1255389.

47. D'Huyvetter M, Vincke C, Xavier C, Aerts A, Impens N, Baatout S, et al. Targeted radionuclide therapy with A 177Lu-labeled anti-HER2 nanobody. Theranostics. 2014;4:708–20. https://doi.org/10.7150/thno.8156.

48. Kameswaran M, Pandey U, Gamre N, Sarma HD, Dash A. Preparation of (177)Lu-Trastuzumab injection for treatment of breast cancer. Appl Radiat Isot. 2019;148:184–90. https://doi.org/10.1016/j.apradiso.2019.04.002.

49. Guleria M, Sharma R, Amirdhanayagam J, Sarma HD, Rangarajan V, Dash A, et al. Formulation and clinical translation of [(177)Lu]Lu-trastuzumab for radioimmunotheranostics of metastatic breast cancer. RSC Med Chem. 2021;12:263–77. https://doi.org/10.1039/d0md00319k.

50. Henning JW, Brezden-Masley C, Gelmon K, Chia S, Shapera S, McInnis M, et al. Managing the risk of lung toxicity with trastuzumab deruxtecan (T-DXd): A canadian perspective. Curr Oncol. 2023;30:8019–38. https://doi.org/10.3390/curroncol30090582.

51. Merrick MJ, Rotsch DA, Tiwari A, Nolen J, Brossard T, Song J, et al. Imaging and dosimetric characteristics of 67 Cu. Phys Med Biol. 2021;66: 035002. https://doi.org/10.1088/1361-6560/abca52.

52. Rasaneh S, Rajabi H, Akhlaghpoor S, Sheybani S. Radioimmunotherapy of mice bearing breast tumors with ^{177}Lu-labeled trastuzumab. Turk J Med Sci. 2012;42(7):1292–8. https://doi.org/10.3906/sag-1105-29.